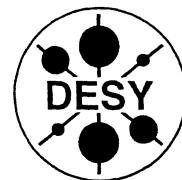


• DP

DEUTSCHES ELEKTRONEN-SYNCHROTRON
in der HELMHOLTZ-GEMEINSCHAFT



DESY 04-057
March 2004

RPC as a Detector for
High Granularity Digital Hadron Calorimetry

V. Ammosov, V. Gapienko, A. Ivanilov, A. Semak,
Yu. Sviridov, E. Usenko, V. Zaets

Institute for High Energy Physics, Protvino, Moscow Region, Russia

F. Sefkow

Deutsches Elektronen-Synchrotron DESY, Hamburg

CERN LIBRARIES, GENEVA



CM-P00047540

ISSN 0418-9833

NOTKESTRASSE 85 - 22607 HAMBURG

RPC as a detector for high granularity digital hadron calorimetry

V. Ammosov^a, V. Gapienko^a, A. Ivanilov^a, F. Sefkow^b, A. Semak^a, Yu. Sviridov^a,
E. Usenko^a, V. Zaets^a

^a*Institute for High Energy Physics, 142281 Protvino Moscow Region, Russia*

^b*DESY, Notkestrasse 85, 22607 Hamburg, Germany*

Abstract

Requirements are formulated for a sampling hadron calorimeter with gaseous active medium and digital read-out as detector component at a future linear e^+e^- -collider. Monogap glass resistive plate chamber (RPC) prototypes equipped with 1 cm^2 readout pads and operated in saturated avalanche and streamer modes are studied as a possible detector for digital hadron calorimetry. Operating characteristics of the prototypes such as induced charges, efficiencies and fired pad multiplicities are measured. Preferable RPC specifications are outlined.

Key words: Hadron calorimetry; Digital read-out; Glass RPC; Saturated avalanche mode; Streamer mode

PACS: 29.40.Cs.

1. Introduction

The physics programme at a future linear e^+e^- -collider (LC) such as TESLA demands the reconstruction of events with multi-jet final states, e.g. di-boson events with hadronic W , Z and Higgs decays, and the identification of the heavy bosons by means of their di-jet invariant mass. Therefore the precise measurement of jet energies is a key factor for success. In particular the sampling hadron calorimeter (HCAL) has to have good imaging capabilities, i.e. sufficient spatial and energy resolution to allow for an efficient separation of individual particle showers in the boosted jets. For transverse shower separation an HCAL cell size well matched to the Moliere radius, R_M , is required. With fine longitudinal sampling this results in a few tens of millions of readout channels, which would make an analogue readout rather expensive. It is there-

fore reasonable to consider a digital readout technique in which the pattern of fired cells is registered in simple *yes/no* mode. Such a digital version of the HCAL (DHCAL) has been proposed as proper option for LC hadron calorimetry (see, for example [1]).

Here, the possible use of resistive plate chambers (RPCs) as active medium is evaluated in a study with small RPC prototypes working in saturated avalanche and streamer mode. Preliminary results on the RPC operation in the streamer mode were reported in [2].

This work was done in the framework of the ECFA/DESY study for a future electron-positron linear collider [3] where calorimetric aspects are investigated in the worldwide CALICE collaboration [4].

2. Optimization of cell size.

The depth of the proposed [1] sampling HCAL is 4.5λ in the barrel and 12.9λ in the end-cap region. The sampling structure is 20 mm (0.12λ) of stainless steel and 6.5 mm for the active layer. The DHCAL active detector should:

- be insensitive to the 4 T magnetic field;
- fit into the thin ($\sim 6\text{ mm}$) active layers;
- be cheap, because the total area of active layers amounts to 6000 m^2

The detector response can be rather slow: the expected rate in the barrel is $< 10^{-4}\text{ Hz/cm}^2$, a rough estimate of the forward end-cap rate is $\sim 10\text{ Hz/cm}^2$.

The cell size of the DHCAL active layer was optimized with respect to energy resolution by means of Monte-Carlo simulations based on GEANT 3.2. The incident particles were charged pions with energies of $2 - 50\text{ GeV}$. The total depth of the simulated calorimeter was 7λ which ensures 98% longitudinal energy containment for these hadron energies. Glass RPCs with 1 mm gas gap filled with tetrafluoroethane ($\text{C}_2\text{H}_2\text{F}_4$) were simulated as active detector. Following the digital approach, the energy was reconstructed from the number of fired cells. A cell was counted to be fired if an energy of at least half of the mean value for a minimum ionizing particle (*MIP*) was deposited in the gas gap within the considered cell area. The resolution was determined taking the nonlinearity of the DHCAL response into account. For comparison, an analogue HCAL (AHCAL) version with 5 mm polystyrene scintillator layers was also simulated.

Fig.1 shows the DHCAL energy resolution as a function of energy for different cell sizes and for the "utmost case", corresponding to infinitesimal granularity where all shower particles with ionization greater than $MIP/2$ are counted.

As the figure shows a DHCAL with a cell area of $1 \times 1\text{ cm}^2$ has a resolution which is close to that obtained in the "utmost" case. The $1 \times 1\text{ cm}^2$ cell size is thus considered to be the optimal choice for the DHCAL active detector. Below 10 GeV the DHCAL with $1 \times 1\text{ cm}^2$ cells has better resolution than the AHCAL. At higher energies the number of fired cells starts to deviate from being proportional

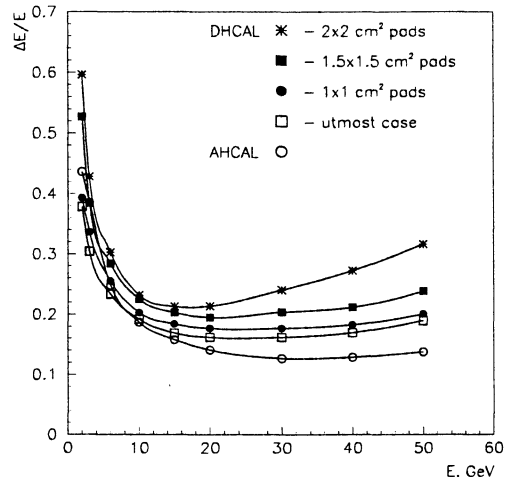


Fig. 1. Hadron energy resolution of the DHCAL as a function of energy for different sizes of read-out cells. The resolution of the AHCAL is also given for comparison.

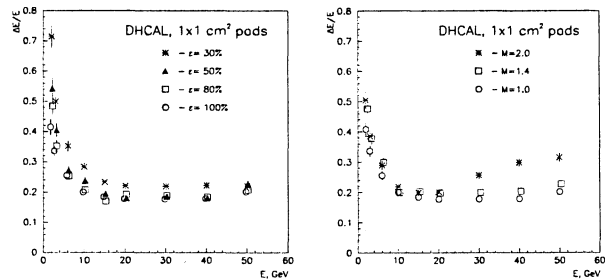


Fig. 2. Energy resolution of the DHCAL as a function of energy: (left) for different efficiencies; (right) for different fired pad multiplicities.

to the energy of the incoming pion. This nonlinearity of the DHCAL response increases with cell size.

The RPCs have so far been assumed to be ideal detectors with 100% efficiency and with only one cell firing per particle crossing its area. In a real RPC some inefficiency may occur, and one discharge can fire several adjacent pads. These effects have been included in the simulation, and figures 2 show how they affect the DHCAL energy resolution. For energies above 6 GeV the resolution is rather insensitive to the efficiency degraded by as much as 50%. At lower energies the numbers

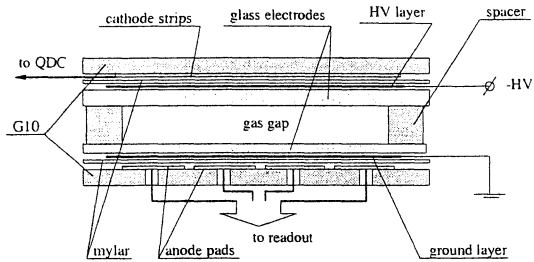


Fig. 3. Schematic cross section of RPC prototypes.

of fired pads are small and statistical fluctuations start to become important.

The energy resolution is not deteriorated as long as the average pad multiplicity M remains below ~ 1.4 . In the simulation of multi-cell response our own experimental distributions of the number of fired channels in the RPC with $1 \times 1 \text{ cm}^2$ pads were used (see below).

3. Prototype design and experimental set-up.

Fig. 3 shows a schematic cross section of the RPC prototypes. The resistive electrodes of our prototypes were made of commercially available glass with resistivity of $\sim 7 \times 10^{12} \Omega \cdot \text{cm}$. The cathode glass plate was 1 mm thick and the anode 0.67 mm . The gaps between glass plates were controlled by PVC buttons of 6 mm diameter glued to the glass. To optimize the prototype performance while keeping the overall detector thickness small, RPCs with gaps of 0.8 , 1.2 , 1.6 and 2.0 mm width were tested. Graphite films of 0.12 mm thickness were glued to the outer surfaces of the cathode and anode for voltage distribution. Negative high voltage was applied to the cathode. For insulation, 0.2 mm thick mylar film was glued to the cathode. One big ($7 \times 7 \text{ cm}^2$) pad on the cathode side was used to measure induced charge, Q . There were 16 anode pads with dimensions of $1 \times 1 \text{ cm}^2$ produced on 1.5 mm thick G10 printed circuit boards (PCB). The whole assembly was inserted into a gas tight aluminum box.

The prototypes were installed in the $5 \text{ GeV}/c$ positive hadron beam at IHEP, Protvino. The beam width (FWHM) was about 4 cm ; several

scintillating counters defined a $2 \times 2 \text{ cm}^2$ trigger area covering four central anode pads. The measurements were carried out also with cosmic rays with a similar set-up. In the avalanche mode signals from 16 anode pads were amplified and discriminated with a 16 channel ATL16 unit[6], and then analyzed by a TDC for efficiency and multiplicity measurements. In the streamer mode signals were sent directly to a discriminator and then to the TDC.

4. Experimental results

The RPC prototypes were tested in two modes of operation: in saturated avalanche and in streamer mode. In both cases tetrafluoroethane, TFE, based gas mixtures were used.

4.1. Saturated avalanche mode

For the saturated avalanche mode [5] mixtures of $C_2H_2F_4/isoC_4H_{10}/SF_6$ with 93/5/2 and 90/5/5 flow rate compositions were used. Four threshold values, 0.6 , 2.2 , 5.0 and 10 mV , were tested to find a compromise between efficiency, ϵ , and multiplicity, M , and to define the requirements for the front-end electronics. The 0.8 mm gas gap was found to be not suited for efficient operation. The efficiency of all other prototypes was measured to be above 98% for a threshold of 2.2 mV corresponding to $\sim 0.35 \text{ pC}$ induced charge. The $\epsilon > 98\%$ HV plateau width is shown as a function of the threshold in Fig.4. Fig.4 shows also voltage value, V_{knee} , at which the 98% efficiency is achieved, as a function of the gap size.

The charge characteristics of the prototypes were typical for the saturated avalanche mode of operation [5]. An example of the charge and multiplicity distributions is shown in Fig.5. The charge distribution is rather wide, with $RMS/\bar{Q} \sim 0.8$. In the whole operating region the average charges do not exceed 6 pC with relatively low tails of larger charges. The pad multiplicity distribution demonstrates that the main contribution to multipad events is due to the case where the induced signal spreads over two adjacent pads ($M = 2$).

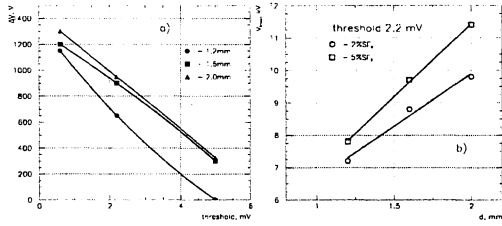


Fig. 4. Saturated avalanche mode: (left) HV plateau width as a function of threshold for different gap sizes; (right) V_{knee} value as a function of gap size for two gas compositions.

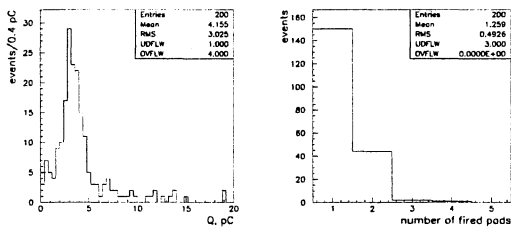


Fig. 5. Charge (left) and multiplicity distribution (right) for an RPC with 1.2 mm gap, operated in avalanche mode, measured at 7.4 kV with gas composition $C_2H_2F_4/isoc_4H_{10}/SF_6 = 93/5/2$; multiplicity for 2.2 mV threshold.

The sharing of the induced signal between neighbouring pads depends on the distance between the head of the avalanche and the read-out pads. Fig.6(left) demonstrates how the mean multiplicity increases with increasing anode insulator thickness t_A . The value $t_A = 0.67$ mm corresponds to the net anode glass without coating, higher t_A values represent cases with additional mylar sheets placed between the anode glass and the PCB. If the applied HV polarity is inverted and the signal read out is on the cathode side with its thicker glass plate, the multiplicity also rises (see Fig.6(right)).

The prototypes were tested at particle incidence angle varying from 0° to 45° . A dependence of the signal characteristics on this angle was not observed. The typical noise rate of the tested prototypes was $(0.1 - 0.8) \text{ Hz/cm}^2$.

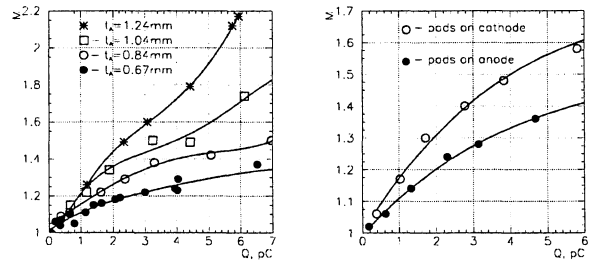


Fig. 6. Mean multiplicity as a function of the induced charge Q for different anode insulator thicknesses t_A (left), and mean multiplicity as a function of Q for two HV polarities (right), for a 1.2 mm gap RPC operated in avalanche mode, measured at 7.4 kV with gas composition $C_2H_2F_4/isoc_4H_{10}/SF_6 = 93/5/2$ and 2.2 mV threshold.

4.2. Streamer mode

For the PC tests in streamer mode we used the following gas mixture: $TFE/isoc_4H_{10}/Ar(N_2)$, in which Ar or N_2 additions were as streamer developers.

An attempt was made to find a mixture with a minimal RMS/\bar{Q} value, which would simplify the DHCAL front-end electronics. A minimal value of $RMS/\bar{Q} = 0.5 - 0.6$ was obtained for $Ar(N_2)$ additions in the $(10 - 20)\%$ range and isobutane additions in the $(10 - 20)\%$ range. The mean charge at V_{knee} increases linearly with the gas gap width.

The discrimination threshold was varied here in the range $(50 - 600) \text{ mV}$ to find a compromise between efficiency and pad multiplicity. The 0.8 mm gas gap was found to be not suited for efficient RPC operation in streamer mode either. The 2 mm gas gap was also inefficient, due to large discharge values and consequently very large recovery times. For the 1.2 mm and 1.6 mm gaps an efficiency of 95% can be reached for a $\sim 1000 \text{ V}$ HV wide plateau, with mean pad multiplicity $\bar{M} = 1.2 - 1.3$. Typical charge and fired pad multiplicity distributions are shown in Fig.7. A narrow one-streamer peak ($FWHM = 20\%$, $\bar{Q} \approx 150 \text{ pC}$) containing 70% of the events is clearly seen. A tail due to multi-streamer discharges, which unfortunately could not be suppressed, leads to an average value of $RMS/\bar{Q} \approx 0.6$ with $\bar{Q} \approx 200 \text{ pC}$. We could

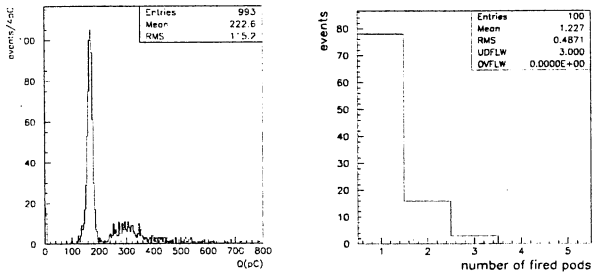


Fig. 7. A 1.2 mm gas gap prototype working in streamer mode: Charge (left) and multiplicity distribution (right), for a prototype with 1.2 mm gap, measured at 7.0 kV with gas composition $C_2H_2F_4/isoC_4H_{10}/Ar = 80/10/10$; multiplicity for 100 mV threshold.

not reach a 100% avalanche to streamer transition, about $\sim 5\%$ of discharges were with very low Q .

The pad multiplicity distribution is similar to the distribution in the saturated avalanche case. For events selected from the single streamer peak region exclusively, the average pad multiplicity is $\bar{M} = 1.15$.

The noise rate was about $(0.10 - 0.15) Hz/cm^2$.

4.3. Avalanche or streamer mode?

In Table 1 we compare the main characteristics of the 1.2 mm prototype working in saturated avalanche and in streamer mode.

The results on efficiency and pad multiplicity are found to be similar for both modes. The essential advantage of the streamer is its strong signal which does not need any amplification. However, streamer discharges with ~ 100 times more charge depositions than for the avalanche lead to larger recovery times which limits the use of the streamer mode for a glass RPC based DHCAL. Fig. 8 shows the efficiency dependence on the counting rate for the 1.6 mm gap RPC operated in avalanche and in streamer mode. The figure shows that the rate capability in streamer mode is only a few Hz/cm^2 , whereas for saturated avalanche mode it is $\sim 100 Hz/cm^2$.

Table 1

Comparison of the 1.2 mm gas gap RPC characteristics for saturated avalanche and streamer mode.

N	Item	avalanche	streamer
1	Working gas mixture	$TFE/IB/SF_6$ = 93/5/2	$TFE/IB/Ar$ = 80/10/10
2	HV working point, kV	~ 7.4	~ 7.4
3	Induced charge Q , pC	3.4	400
4	σ_Q/Q	0.9	0.6
5	Threshold/50 Ω , mV	2	300
6	Efficiency, %	98	95
7	HV plateau width, kV	0.65	1.0
8	Pad multiplicity	1.35	1.25
9	Noise rate, Hz/cm^2	0.7	0.1
10	Rate capability, Hz/cm^2	100	few

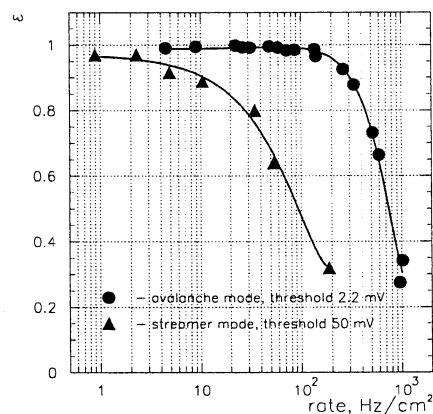


Fig. 8. Efficiency as a function of rate for 1.6 mm RPC operated in streamer and avalanche mode.

5. Conclusion

An optimization study was carried out to evaluate the possible use of RPCs with small read-out pads as active medium for a LC DHCAL. An optimal pad size, with respect to energy resolution, was estimated by means of MC simulations to be $1 \times 1 cm^2$. The performance of mono-gap glass RPC prototypes with $1 \times 1 cm^2$ anode read-out pads was studied in saturated avalanche and streamer mode.

In both modes the chambers show good efficiency ($> 95\%$) and low pad multiplicity per registered track (< 1.4). Our simulation results show that the deterioration in energy resolution caused by RPC inefficiencies and by multi-pad response is rather small for the performance figures of our prototype RPCs.

Comparing both operation modes we conclude that the saturated avalanche mode is to be preferred mostly because of its higher rate capability and safer operation.

As the result of this study, preferable RPC specifications are seen as follows:

- mono-gap glass chamber as the simplest and most robust choice;
- size of the gas gap = $1.2 - 1.6 \text{ mm}$;
- operation in saturated avalanche mode;
- $TFE/isoC_4H_{10}/SF_6$ gas mixture with $\sim 5\%$ of isobutane and few % of SF_6 as working composition;
- system of $1 \times 1 \text{ cm}^2$ pads on the anode side;
- a resistive anode plate as thin as possible;
- signal discrimination threshold of $\sim 2 \text{ mV}$;

Acknowledgements

We wish to thank deeply A. Golovin for his efforts in manufacturing the RPC prototypes. The authors are grateful to the CALICE Collaboration members, especially to J-C. Brient, M. Danilov, R-D. Heuer, V. Korbelt, J. Repond and H. Videau for their valuable discussions and remarks.

This work was partially supported by the ECFA/DESY fund and by the Russian Integracia fund, grant No. I0717/1652.

References

- [1] TESLA Technical Design Report, part4: A detector for TESLA, DESY 2001-011; ECFA 2001-209; TESLA report 2001-23; TESLA-FEL 2001-05, March 2001.
- [2] V.Ammosov, Nucl. Instr. Meth., Vol. **A494**, 355(2002).
- [3] <http://www.desy.de/conferences/ecfa-desy-lcext.html>
- [4] http://polywww.in2p3.fr/flc/calor_LC.html

- [5] V.Koreshev et al., Nucl. Instr. Meth., Vol. **A456**, 45(2000).
- [6] E.Usenko, IHEP preprint 2001-53, Protvino, 2001.